



# On the Parameters Investigation of a Non-Intrusive Multiscale Framework for Structural Analysis

Neimar A. da Silveira Filho<sup>1</sup>, Felício B. Barros<sup>1</sup>

<sup>1</sup>*Dept. of Structural Engineering, Federal University of Minas Gerais  
Av. Presidente Antônio Carlos, 31270-901, Minas Gerais, Brazil  
neimarsilveira@ufmg.br, feliciobarros@gmail.com*

**Abstract.** IGL-GFEM<sup>gl</sup> is a multiscale framework proposed by H. Li, P. O'Hara, and C. A. Duarte in 2021 that combines the IGL strategy with the GFEM<sup>gl</sup>. In the Iterative Global-Local method (IGL), two different meshes are adopted. The global mesh is used to describe the global behavior of the structure. Local features are represented in the local mesh. The solution of the two meshes is coupled through a non-intrusive iterative algorithm that exchanges displacements and enforces the equilibrium between them. The GFEM<sup>gl</sup> considers two scales of representations, but the coupling is provided by the GFEM's enrichment strategy. Finally, in the IGL-GFEM<sup>gl</sup> framework, a third problem is defined, named mesoscale. The mesoscale works as a bridge between the two methods (IGL and IGL-GFEM<sup>gl</sup>), allowing a non-intrusive coupling of the global problem FEM solution and the meso-local scale solution provided by the GFEM<sup>gl</sup>. In this work, the commercial software Abaqus solves the global problem and is coupled with an in-house computational platform where GFEM<sup>gl</sup> is already implemented. A thorough investigation is performed over some IGL-GFEM<sup>gl</sup> parameters, such as the size of the mesoscale and the use of acceleration techniques to improve the convergence of the method.

**Keywords:** Generalized Finite Element Method, Global-Local Analysis, Non-intrusive coupling, Multiscale analysis

## 1 Introduction

In the industry, engineers mostly count on commercial software thanks to their certifications for specific use along with computation efficiency. However, even these pieces of software might not be capable of handling spatial multiscale problems. Problems involving singularities, discontinuities, complex geometries, and localized deformations, although commonly faced in the engineering applications, often challenge the formulation of the Finite Element Methods (FEM). Modeling this class of problems can be burdensome or even not possible when using FEM, and significant errors may be incorporated in the approximate solution [1, 2].

Due to recent advances in parallel computation, instead of embedding all the information in one massive model, there is a trend to break problems of this class into smaller and more detailed ones [3]. Consequently, this approach requires strategies to couple the results of all scales. These strategies are referred to as coupling methods, which may be classified according to their intrusiveness level. A coupling method is more intrusive as its implementation requires deeper modification of the involved solvers. When commercial software is involved, non-intrusive algorithms are more appealing as code modification is generally not feasible.

Naturally, coupling between FEM and other numerical methods that overcome some of its limitations has been investigated in the past few years. The Generalized Finite Element Method (GFEM) [4–9] and the Generalized Finite Element Method with global-local enrichment functions (GFEM<sup>gl</sup>) [10, 11] are examples of this class of methods. It is noteworthy that GFEM formulation is considered equivalent to the eXtended Finite Element Method (XFEM) [12] and hereon the G/XFEM notation will be held. The G/XFEM has been successfully applied to solve complex problems in the past decades. Due to some of its advantages over FEM [13], G/XFEM has drawn attention and has recently been implemented in commercial finite element programs [14]. The GFEM<sup>gl</sup> implementations, on

the other hand, remain restricted to research software so far and it is not available in program suites with industrial appeal.

Considering the interesting features of non-intrusive coupling, Li, O'Hara and Duarte [15] recently proposed a non-intrusive implementation of the GFEM<sup>gl</sup>. In this approach, the problem is divided into three scales. The global scale may be solved by FE analysis. The GFEM<sup>gl</sup> approach is used at meso and local scales. Coupling between FEM and GFEM<sup>gl</sup> results is performed through the Iterative Global-Local (IGL), a highly non-intrusive algorithm proposed by Whitcomb [16]. This non-intrusive implementation of the GFEM<sup>gl</sup> is referred to as IGL-GFEM<sup>gl</sup>.

The IGL-GFEM<sup>gl</sup> is a brand-new strategy that provides a framework for the combination of industrial software with the GFEM<sup>gl</sup>. As far as the authors are aware, there is no work investigating the influence of the IGL-GFEM<sup>gl</sup>'s parameters on its approximate solution. This paper presents new investigations under the IGL-GFEM<sup>gl</sup>. In this sense, the strategy was implemented to couple Abaqus and INSANE, an open-source software developed at the Federal University of Minas Gerais which implements the GFEM<sup>gl</sup> [17–20]. Tests were performed in order to study the following parameters: (a) tolerance of the IGL's convergence criterion, (b) number of GFEM<sup>gl</sup> iterations, (c) size of the mesoscale domain, and (d) use of convergence acceleration techniques.

## 2 The IGL-GFEM<sup>gl</sup> framework

### 2.1 A non-intrusive coupling method: Iterative Global Local

The Iterative Global-Local [16] is a non-intrusive coupling procedure based on the exchange of displacements and forces between models. Although originally design for FE analysis, it can be easily implemented for other methods. Figure 1 presents a reference problem for the presentation of the IGL. The global model concerns the whole domain  $\bar{\Omega} = \bar{\Omega}_L \cup \bar{\Omega}_C$ , where  $\bar{\Omega}_L$  is the local domain and  $\bar{\Omega}_C$  is its complement regarding  $\bar{\Omega}$ . Then, the interface between global subdomains is defined as  $\Gamma = \bar{\Omega}_L \cap \bar{\Omega}_C$ .

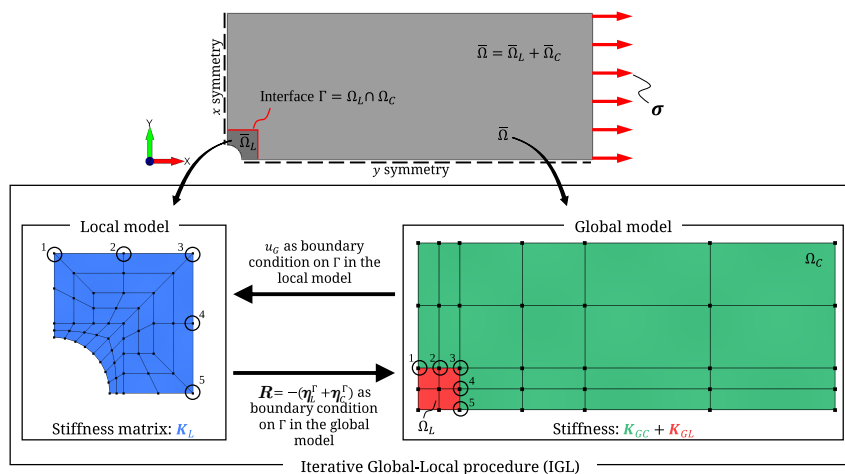


Figure 1. The Iterative Global-Local (IGL) procedure.

The initial approximated solution to the global problem can be computed from

$$(\mathbf{K}_{GC} + \mathbf{K}_{GL}) \cdot \tilde{\mathbf{u}}_G = \mathbf{f}_G, \quad (1)$$

and the solution  $\tilde{\mathbf{u}}_G$  is then applied as prescribed displacement on the interface  $\Gamma$  of the local model. The local solution can be computed from the system of equations of the local problem

$$\mathbf{K}_L \cdot \tilde{\mathbf{u}}_L = \mathbf{f}_L. \quad (2)$$

Once it was supposed that  $\mathbf{K}_{GL} \neq \mathbf{K}_L$ , we can assume that  $\bar{\Omega}_L$  is not equally represented in eqs. (1) and (2). Therefore the forces balance on  $\Gamma$  is not satisfied.

The IGL algorithm seeks to reduce these unbalanced forces by an iterative procedure. The idea is to compute the forces at  $\Gamma$  in the complementary domain of the global model,  $\eta_{GC}^\Gamma$ , and compare it with  $\eta_L^\Gamma$ , the forces on  $\Gamma$  in

the local model. The difference between these two vectors is called residual forces. The associated reaction vector  $\mathbf{R}$  is applied as a correction on  $\Gamma$  in the global problem. The updated global model can now be solved again, and this process continues until a convergence criterion is satisfied. In conclusion, the IGL algorithm has the following steps [15], that were schematically represented in fig. 1:

**Step 1** *Global solution*:  $\tilde{\mathbf{u}}_G$  is obtained by eq. (1).

**Step 2** *Local solution*:  $\tilde{\mathbf{u}}_L$  is obtained by eq. (2) using  $\tilde{\mathbf{u}}_G$  as prescribed displacements at the interface  $\Gamma$ .

**Step 3** *Residual forces computation*:  $\tilde{\mathbf{u}}_G$  and  $\tilde{\mathbf{u}}_L$  are used to compute the reactions at  $\Gamma$  in  $\tilde{\Omega}_G$  and  $\tilde{\Omega}_L$ , respectively. The residual forces vector  $\mathbf{R}$  is computed by

$$\mathbf{R} = -(\boldsymbol{\eta}_L^\Gamma + \boldsymbol{\eta}_{GC}^\Gamma) = -[(\mathbf{K}_L \cdot \tilde{\mathbf{u}}_L - \mathbf{f}_L) + (\mathbf{K}_{GC} \cdot \tilde{\mathbf{u}}_{GC} - \mathbf{f}_{GC})] |_\Gamma, \quad (3)$$

**Step 4** *Global load vector correction*: the residual vector  $\mathbf{R}$  is added to the global model load vector.

**Step 5** *Iteration*: go back to Step 1 until the convergence criterion is satisfied.

Li, O'Hara and Duarte [15] proposed the  $L^2$ -norm of the residual vector  $\mathbf{R}$  as a convergence measure for the IGL. Then, a tolerance  $\epsilon$  is arbitrarily chosen and the convergence criteria is satisfied when, at the iteration  $k$ ,

$$\frac{\|\mathbf{R}^k\|}{\|\mathbf{R}^0\|} < \epsilon, \quad (4)$$

where  $\mathbf{R}^0$  is the residual of the first iteration.

The IGL procedure may be presented in an incremental form [3, 21], which implies that the algorithm is a modified Newton method. Therefore, it can benefit from the acceleration techniques developed over the years for this class of problem to overcome convergence limitations. In this work, two of those techniques were evaluated, namely the *static* [22] and the *dynamic relaxation* [23].

## 2.2 IGL-GFEM<sup>gl</sup> for the solution of multi-scale problems

In a recent work, Li, O'Hara and Duarte [15] presented a solution strategy combining IGL and GFEM<sup>gl</sup>, hereon called IGL-GFEM<sup>gl</sup>. Figure 2 presents the workflow of the method, in which the problem is divided into three scales. The global scale covers the whole problem and there is no concern with modeling local features, and the associated mesh is usually coarse. Regions where local behaviors are expected define the local scale. Finally, the mesoscale is an intermediate scale bridging global and local scale. The mesoscale is a subregion of the global scale that contains the local features but neglects them, so its mesh will be similar to the global model. The mesoscale work as the local scale of the IGL and the global scale of the GFEM<sup>gl</sup>. Information exchange between global and meso scales are provided by IGL. As those scales are supposed to have matching meshes, this process is performed exactly as proposed by Whitcomb [16]. On the other hand, meso and local scale are solved using GFEM<sup>gl</sup> strategy.

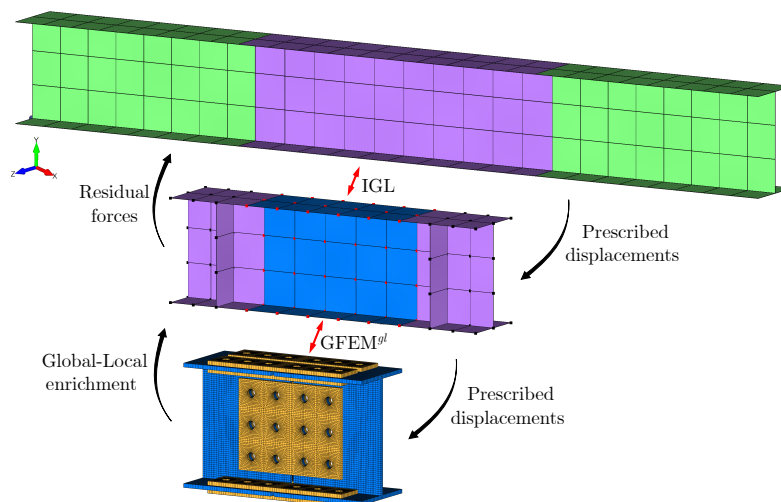


Figure 2. Iterative Global Local solution applied to the G/XFEM with global-local enrichment.

### 3 Numerical Results

The investigation of the IGL-GFEM<sup>gl</sup> parameters is now presented through a set of numerical simulations of elastic linear problems. It is worthy to mention that the IGL-GFEM<sup>gl</sup> implementation was validated by standard FE analysis using very fine meshes [24]. Figure 3 presents the problem used in this section. A plate with a central square hole is loaded under plane stress condition. The problem behavior is linear elastic and the orifice is the only local feature. The elasticity modulus is  $E = 2 \cdot 10^{11}$  in consistent units (c.u.) and the Poisson's ratio is  $\nu = 0.30$ .

The three models used in IGL-GFEM<sup>gl</sup> are built with linear quadrilateral elements Q4. For the global and meso models, a regular mesh was defined with elements of the same size of the hole, i.e., 5.0. The local model has mesh size of 2.5. The adopted meshes are also presented in Figure 3. The three models have together 690 degrees of freedom. For comparison, two FE models were defined: Model A with mesh size of 2.5 – equivalent to the one used in the local scale – with 1,064 degrees of freedom; Model B, providing a reference solution, with mesh of size 0.625 and 15,680 degrees of freedom.

**Tolerance  $\epsilon$ .** To investigate the influence of the tolerance in the IGL-GFEM<sup>gl</sup> solution, the problem from Figure 3 was solved using five distinct values of  $\epsilon$ :  $10^{-2}$ ,  $10^{-3}$ ,  $10^{-5}$ ,  $10^{-7}$  and  $10^{-10}$ . Figure 4 presents a plot comparing the results in terms of strain components, indicating insignificant change in IGL-GFEM<sup>gl</sup> results when  $\epsilon < 10^{-5}$ .

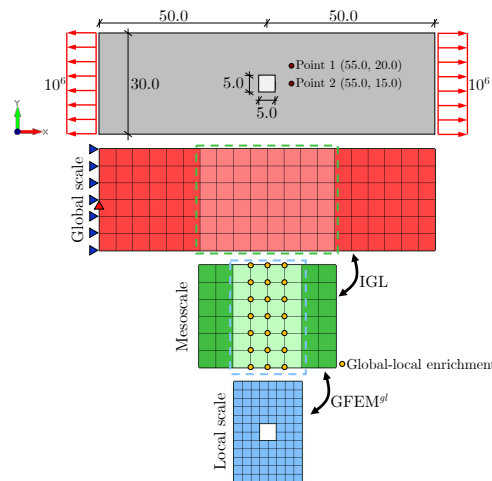


Figure 3. Definition of the problem and IGL-GFEM<sup>gl</sup> models (consistent units).

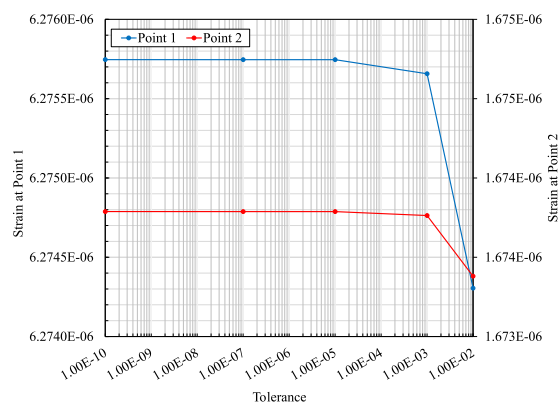


Figure 4. Strain components at Points 1 and 2 for different  $\epsilon$ .

**GFEM<sup>gl</sup> iterations.** Li, O'Hara and Duarte [15] suggest one GFEM<sup>gl</sup> iteration ( $n_{GL} = 1$ ) for most problems. Despite that, there is still interest in investigate how  $n_{GL}$  affects the IGL-GFEM<sup>gl</sup> solution. In the GFEM<sup>gl</sup>, the global-local enrichment changes the shape functions of the global model – which in the scope of the IGL-GFEM<sup>gl</sup> is the mesoscale model. Hence, the stiffness matrix of the mesoscale is modified by the global-local enrichment. The convergence rate of the IGL procedure depends on the stiffness gap between the models, i.e., global and meso model in the scope of the IGL-GFEM<sup>gl</sup>. In this sense, it is worth investigating the influence of  $n_{GL}$  in the IGL convergence. The problem presented in fig. 3 was then solved using  $n_{GL} = 1, 2, 3,$  and  $6$ .

Table 1 compares the relative residual force (see eq. 4) at each IGL iteration for different values of  $n_{GL}$ . Despite the slight change in the results when  $n_{GL}$  goes from 1 to 2, the number of GFEM<sup>gl</sup> iterations does not seem to impact the quality of the IGL-GFEM<sup>gl</sup> for this class of problem. The same can be stated regarding the converge behavior of the framework. In this sense, Li et al. [15] recommendation for using  $n_{GL} = 1$  seems to a good choice as  $n_{GL}$  has a great impact on the execution time [21].

**Mesoscale.** The model defined in fig. 3 was derived into three versions, as show in fig. 5. The only difference between them is the mesoscale extension. Model M1 is equivalent to the original model. Model M2 has only one layer of elements between the global-meso interface and the local domain, whereas Model M3 has no elements in this region, i.e., the mesoscale and local domain cover the exact same region.

We now take the execution time of Model M1 as reference, i.e. its relative execution time is 1.0. The model M2 provided the fastest solution, at a mark of 0.981. Both M1 and M2 solutions needed six IGL iterations until

Table 1. IGL-GFEM<sup>gl</sup> convergence for different  $n_{GL}$ .

IGL iteration	Relative residual force			
	$n_{GL} = 1$	$n_{GL} = 2$	$n_{GL} = 3$	$n_{GL} = 6$
0	1.0000E+00	1.0000E+00	1.0000E+00	1.0000E+00
1	6.2556E-02	6.2526E-02	6.2524E-02	6.2524E-02
2	3.8612E-03	3.8620E-03	3.8618E-03	3.8618E-03
3	2.3807E-04	2.3829E-04	2.3827E-04	2.3827E-04
4	1.4677E-05	1.4701E-05	1.4700E-05	1.4700E-05
5	9.0486E-07	9.0697E-07	9.0686E-07	9.0688E-07

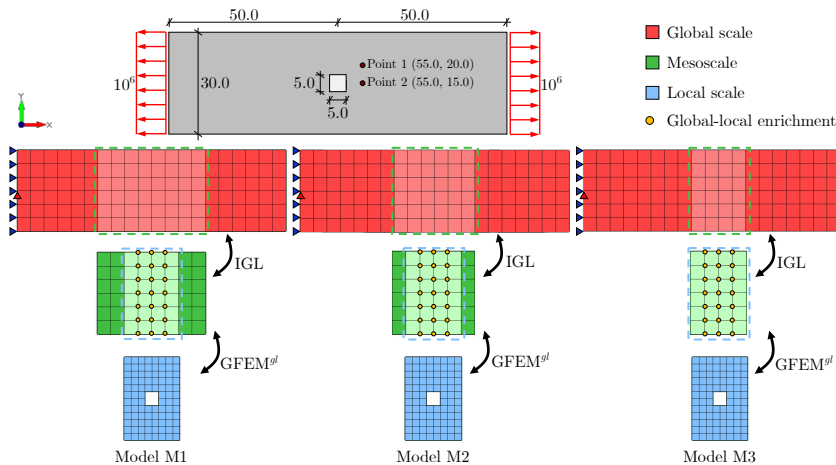


Figure 5. Models regarding mesoscale size investigation (consistent units).

convergence, however, M2 was a little bit faster as its mesoscale is reduced compared with M1. For model M3, the results indicate the opposite as the relative execution time is 1.250. The solution time increased in comparison to M1 even though the mesoscale is smaller in M3. This is explained by the increase in number of iterations required until convergence, as M3 performs eight IGL iterations. The mesoscale size impacts on the convergence of the IGL-GFEM<sup>gl</sup>. As illustrated by the fig. 6a, the convergence rate gets slower as the layers of elements between the local domain and the global-meso interface is reduced. Even though the position of  $\Gamma$  is different in each model, it does not affect the solution quality, as shown in fig. 6b.

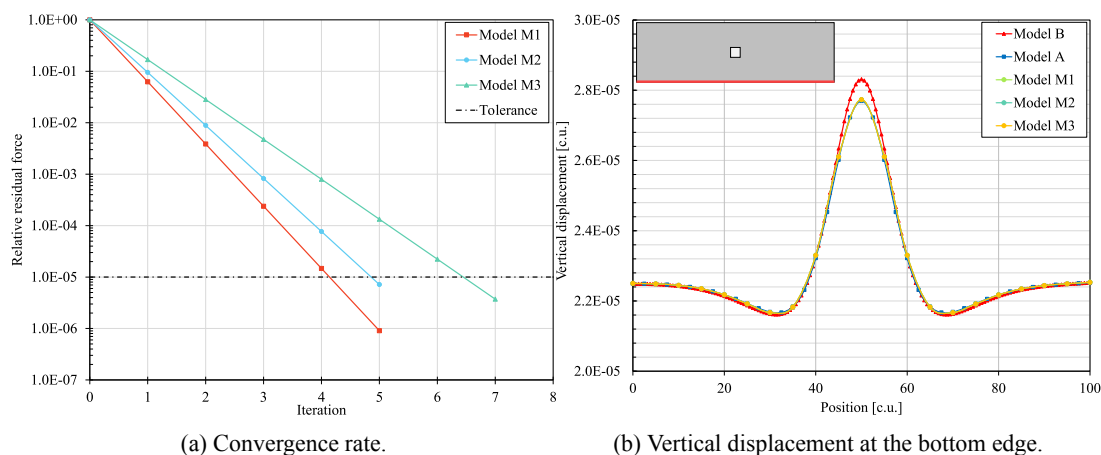


Figure 6. Results of models M1, M2 and M3.

**Acceleration techniques.** In the scope of the IGL-GFEM<sup>gl</sup>, the IGL procedure diverges if the mesoscale model is sufficiently stiffer than global model. In order to enforce this scenario, the problem from fig. 3 was modified so the elasticity modulus of the meso and local models, denoted  $E_M$ , is set to be greater than  $E$ .

The static relaxation [22] was applied for the case when  $E_M = 3.0E$ . Various values of the relaxation factor  $\omega$  were used. We should first note that for  $\omega = 1.0$ , which is equivalent to the standard solution, the solution does not converge. Although the static relaxation improved convergence, as per fig. 7a, its performance depends highly on the value of  $\omega$ . In addition, the fact that  $\omega$  holds the same value throughout the entire analysis is a limitation in itself. The dynamic relaxation [23] overcomes these limitations.

Figure 7b plots the convergence rate using dynamic relaxation for the solution of a set of ratios  $E_M/E$ . For  $E_M = 3.0E$ , we note that convergence is closer to the best result obtained using static relaxation. In fact, over the iterations, the value of  $\omega^k$  tends to 0.35. Figure 7b also shows that, for a given problem, the convergence rate is not influenced by the ratio  $E_M/E$  when the dynamic relaxation is employed.

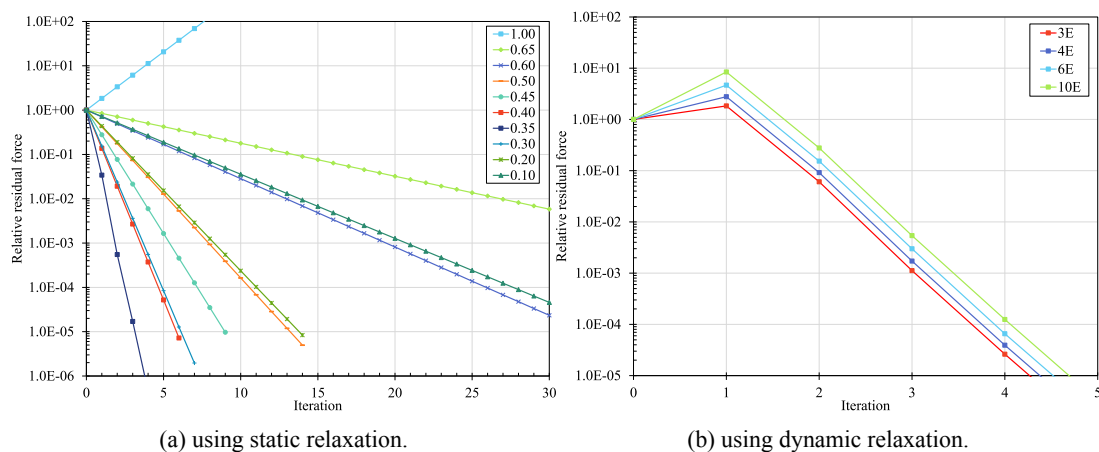


Figure 7. Convergence of the IGL-GFEM<sup>gl</sup> with acceleration techniques.

## 4 Conclusions

This paper briefly presented a parameter investigation of the IGL-GFEM<sup>gl</sup> regarding elastic linear problems. We highlight the influence of mesoscale extension on IGL-GFEM<sup>gl</sup> performance. In terms of solution accuracy, the results suffered very little influence of the number of element layers between the local domain and the global-meso interface  $\Gamma$ . Nevertheless, numerical simulations found a trade-off relationship between the mesoscale size and the computational cost of the solution. While models with reduced mesoscale can be solved faster, the IGL convergence rate is significantly slower when the  $\Gamma$  is too close to the local domain. In addition, for the class of problem under study, the results indicate that the dynamic relaxation reduces the relevance of the stiffness gap between the global and mesoscales in solution convergence rate.

**Acknowledgements.** The authors gratefully acknowledge the important support of the Brazilian research agencies FAPEMIG (in Portuguese “Fundação de Amparo à Pesquisa de Minas Gerais” – Grant APQ-01656-18), CNPq (in Portuguese “Conselho Nacional de Desenvolvimento Científico e Tecnológico” - Grant 308444/2022-1) and CAPES (in Portuguese “Coordenação de Aperfeiçoamento de Pessoal de Nível Superior”).

**Authorship statement.** The authors hereby confirm that they are the sole liable persons responsible for the authorship of this work, and that all material that has been herein included as part of the present paper is either the property (and authorship) of the authors, or has the permission of the owners to be included here.

## References

- [1] V. Gupta, C. Duarte, I. Babuška, and U. Banerjee. Stable GFEM (SGFEM): Improved conditioning and accuracy of GFEM/XFEM for three-dimensional fracture mechanics. *Computer Methods in Applied Mechanics and Engineering*, vol. 289, pp. 355–386, 2015.



- [2] E. Béchet, H. Minnebo, N. Moës, and B. Burgardt. Improved implementation and robustness study of the X-FEM for stress analysis around cracks. *International Journal for Numerical Methods in Engineering*, vol. 64, n. 8, pp. 1033–1056, 2005.
- [3] M. Duval, J.-C. Passieux, M. Salaün, and S. Guinard. Non-intrusive Coupling: Recent Advances and Scalable Nonlinear Domain Decomposition. *Archives of Computational Methods in Engineering*, vol. 23, n. 1, pp. 17–38, 2014.
- [4] I. Babuška, G. Caloz, and J. E. Osborn. Special finite element methods for a class of second order elliptic problems with rough coefficients. *SIAM Journal on Numerical Analysis*, vol. 31, pp. 945–981, 1994.
- [5] J. Melenk and I. Babuška. The partition of unity finite element method: Basic theory and applications. *Computer Methods in Applied Mechanics and Engineering*, vol. 139, n. 1–4, pp. 289–314, 1996.
- [6] T. Strouboulis, I. Babuška, and K. Copps. The design and analysis of the Generalized Finite Element Method. *Computer Methods in Applied Mechanics and Engineering*, vol. 181, n. 1–3, pp. 43–69, 2000.
- [7] C. Duarte and J. T. Oden. Hp clouds – a meshless method to solve boundary-value problem. Technical Report TICAM Report 95-05 (Revised), Texas Institute for Computational and Applied Mathematics, 1995.
- [8] C. A. Duarte. *The hp cloud method*. Phd dissertation, University of Texas at Austin, Austin, Texas, United States of America, 1996.
- [9] C. Armando Duarte and J. Tinsley Oden. H-p clouds - an h-p meshless method. *Numerical Methods for Partial Differential Equations*, vol. 12, n. 6, pp. 673–705, 1996.
- [10] C. Armando Duarte, D.-J. Kim, and I. Babuška. A Global-Local Approach for the Construction of Enrichment Functions for the Generalized FEM and Its Application to Three-Dimensional Cracks. *Advances in Meshfree Techniques*, pp. 1–26, 2007.
- [11] C. Duarte and D.-J. Kim. Analysis and applications of a generalized finite element method with global–local enrichment functions. *Computer Methods in Applied Mechanics and Engineering*, vol. 197, n. 6–8, pp. 487–504, 2008.
- [12] T. Belytschko, R. Gracie, and G. Ventura. A review of Extended/Generalized Finite Element Methods for material modelling. *Modelling and Simulation in Materials Science and Engineering*, vol. 17, pp. 043001, 2009.
- [13] P. Gupta, J. Pereira, D.-J. Kim, C. Duarte, and T. Eason. Analysis of three-dimensional fracture mechanics problems: A non-intrusive approach using a generalized finite element method. *Engineering Fracture Mechanics*, vol. 90, pp. 41–64, 2012.
- [14] M. Smith. *ABAQUS/Standard User's Manual, Version 6.14*. Dassault Systèmes Simulia Corp, 2016.
- [15] H. Li, P. O'Hara, and C. Duarte. Non-intrusive coupling of a 3-D Generalized Finite Element Method and Abaqus for the multiscale analysis of localized defects and structural features. *Finite Elements in Analysis and Design*, vol. 193, pp. 103554, 2021.
- [16] J. Whitcomb. Iterative global/local finite element analysis. *Computers & Structures*, vol. 40, n. 4, pp. 1027–1031, 1991.
- [17] F. T. Fonseca and R. L. Pitangueira. An object oriented class organization for dynamic geometrically non-linear. In *Iberian-Latin-American Congress on Computational Methods in Engineering (CILAMCE)*, 2007.
- [18] R. L. S. Pitangueira, F. T. Fonseca, J. S. Fuina, L. Camara, R. L. Ferreira, R. N. Moreira, S. S. Penna, S. S. Saliba, and M. T. Fonseca. INSANE - versão 2.0. In *Iberian-Latin-American Congress on Computational Methods in Engineering (CILAMCE)*, 2008.
- [19] P. D. Alves. Estratégias global-local aplicadas ao método dos elementos finitos generalizados. Master's dissertation, Federal University of Minas Gerais (UFMG), Belo Horizonte, MG, Brazil, 2012.
- [20] G. M. Fonseca. Propagação de trincas em meios elásticos lineares via método dos elementos finitos generalizados com estratégia global-local automatizada. Master's dissertation, Federal University of Minas Gerais (UFMG), Belo Horizonte, MG, Brazil, 2019.
- [21] N. A. Silveira Filho. Implementação não intrusiva do Método dos Elementos Finitos Generalizados com enriquecimento Global-Local. Master's dissertation, Federal University of Minas Gerais Federal de Minas Gerais (UFMG), Belo Horizonte, MG, Brazil, 2023.
- [22] R. V. Southwell. *Relaxation Methods in Engineering Science*. Oxford University Press, 1940.
- [23] B. M. Irons and R. C. Tuck. A version of the Aitken accelerator for computer iteration. *International Journal for Numerical Methods in Engineering*, vol. 1, n. 3, pp. 275–277, 1969.
- [24] N. A. Silveira Filho and F. B. Barros. Implementation of a non-intrusive approach using a global-local strategy for the Generalized Finite Element Method. In *XLIII Iberian-Latin-American Congress on Computational Methods in Engineering (CILAMCE)*, 2022.